



ISTITUTO NAZIONALE DI RICERCA METROLOGICA Repository Istituzionale

Control of bulk superconductivity in a BCS superconductor by surface charge doping via electrochemical gating

This is the author's submitted version of the contribution published as:

Original

Control of bulk superconductivity in a BCS superconductor by surface charge doping via electrochemical gating / Piatti, E.; Daghero, D.; Ummarino, G. A.; Laviano, F.; Nair, J. R.; Cristiano, R.; Casaburi, A.; Portesi, C.; Sola, A.; Gonnelli, R. S. - In: PHYSICAL REVIEW. B. - ISSN 2469-9950. - 95:14(2017).
[10.1103/PhysRevB.95.140501]

Availability:

This version is available at: 11696/57271 since: 2021-03-04T17:45:08Z

Publisher:

American Physical Society

Published

DOI:10.1103/PhysRevB.95.140501

Terms of use:

This article is made available under terms and conditions as specified in the corresponding bibliographic description in the repository

Publisher copyright

American Physical Society (APS)
Copyright © American Physical Society (APS)

(Article begins on next page)

Control of bulk superconductivity in a BCS superconductor by surface charge doping via electrochemical gating

E. Piatti,¹ D. Daghero,¹ G. A. Ummarino,¹ F. Laviano,¹ J. R. Nair,¹ R. Cristiano,² A. Casaburi,³ C. Portesi,⁴ A. Sola,⁴ and R. S. Gonnelli^{1,*}

¹*Department of Applied Science and Technology, Politecnico di Torino, Torino, Italy*

²*CNR-SPIN Institute of Superconductors, Innovative Materials and Devices, UOS-Napoli, Napoli, Italy*

³*School of Engineering, University of Glasgow, Glasgow, UK*

⁴*INRIM - Istituto Nazionale di Ricerca Metrologica, Torino, Italy*

(Dated: July 10, 2016)

The electrochemical gating technique is a powerful tool to tune the surface conduction properties of various materials by means of pure charge doping – even inducing surface superconductivity in insulators or semiconductors – but its efficiency is generally thought to be hampered in materials with a good electronic screening. Nevertheless, if applied to a bulk metallic superconductor (NbN), this approach allows observing a reversible enhancement or suppression of the *bulk* superconducting transition temperature, depending on the sign of the gate voltage. These results can be interpreted in terms of proximity effect, and indicate that the effective screening length depends on the induced charge density, becoming much larger than that expected at very high electric fields.

The field effect (i.e. the modulation of the conduction properties of a material by means of a static transverse electric field) is widely used in semiconducting electronic devices, namely FETs. Recently, unprecedented intensities of the electric field – and thus densities of induced charge – have been reached by exploiting the formation of an electric double layer (EDL) at the interface between an electrolyte and the solid, when a voltage is applied between the latter and a gate electrode immersed in the electrolyte. The EDL acts as a nanoscale capacitor with a nanometric spacing between the “plates”, so that the electric field can be orders of magnitude higher than in standard field-effect (FE) devices. In these extreme conditions, new phases (including superconductivity) have been discovered in various materials, mostly semiconducting or insulating in their native state [1–5]. Instead, high-carrier-density systems such as metals and standard BCS superconductors have so far received little attention, because the electronic screening strongly limits the FE. To the best of our knowledge, a few works on gold [6, 7] and other noble metals [8] remain the only literature about EDL gating on normal metals.

The field effect on BCS superconductors was investigated in the Sixties via solid dielectric [9] and ferroelectric [10] gating, and small (positive or negative) variations of the superconducting transition temperature (T_c) were observed on increasing/decreasing the charge carrier density. Similar results were recently obtained by EDL gating in Nb [11] thin films. In this case completely reversible T_c shifts were observed, about three orders of magnitude larger than in [9, 10], though still smaller than 0.1 K. Despite the very effective electronic screening expected close to T_c (and due to unpaired electrons) the suppression of T_c was visible also in films as thick as 120 nm. This means that the superconducting properties of the *bulk* were somehow changed by the applied gate voltage; otherwise, the surface layer with reduced T_c would

have been shunted by the underlying bulk giving no visible effect on the transition. A proper understanding of how this could happen is however still lacking [11].

In this work we solve this problem – that has been open for 50 years – by systematically studying the T_c modulation of NbN thin films under EDL gating for different values of the film thickness t . We find that the T_c shift does depend on t , thus proving that the whole bulk comes into play. We show that, if the proximity effect is taken into account in the strong-coupling limit of the standard BCS theory, this finding turns out to be compatible with a charge induction limited to the surface. Interestingly, the effective electrostatic screening length (EESL) increases with the induced charge, finally becoming much higher than the Thomas-Fermi screening length λ_{TF} in the normal state.

NbN thin films were grown on insulating MgO substrates by reactive magnetron sputtering. The device geometry was defined by photolithography and subsequent wet etching in a 1:1 HF:HNO₃ solution. The inset to Fig. 1a shows the scheme of the samples: the strip is 135 μm wide, with current pads on each end and four voltage contacts on each side, spaced by 946 μm from one another. This geometry allows measuring the voltage drop across different portions of the strip at the same time, and thus defining both an *active* (gated) and a *reference* (ungated) channel.

The thickness t of the film was measured by atomic force microscopy (AFM). Fig. 1a shows the sheet resistance R_{\square} vs temperature of the pristine film ($t = 39.2 \pm 0.8$ nm). The non-monotonic behavior of $R_{\square}(T)$ and the residual resistivity ratio $RRR = R(300\text{K})/R(16\text{K}) = 1.05$ are characteristic of granular NbN films of fairly high quality [12]. Subsequent steps of Ar-ion milling were used to progressively reduce the film thickness to 27.1 ± 1.5 nm, 18.3 ± 2.3 nm and finally 9.5 ± 3.0 nm (see Supplementary Information for further details). On reducing

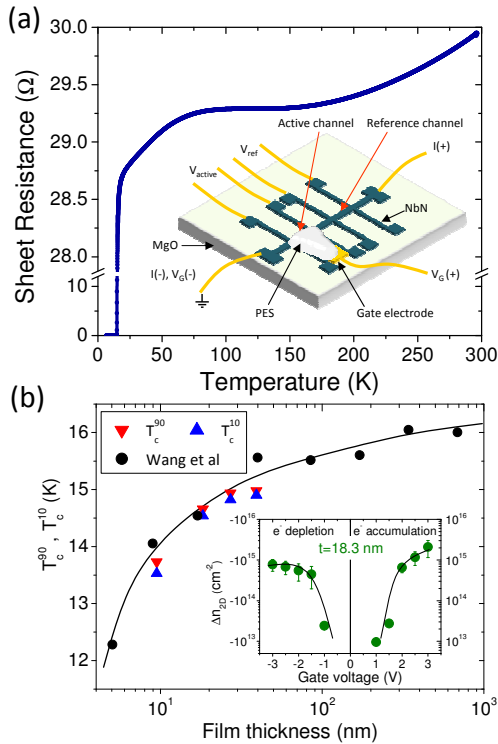


FIG. 1: (a) Sheet resistance as a function of temperature for the pristine 39.2 nm-thick device (prior to the PES deposition). The inset shows a schematic of the complete device. (b) Transition temperature as a function of thickness for our devices: both T_c^{90} (down triangles) and T_c^{10} (up triangles) are reported to show the variation in the transition width. Black dots are data taken from literature [15]. Inset: typical Δn_{2D} vs. V_G curve determined by chronocoulometry.

t , the T_c was progressively reduced (in good agreement with the curve for NbN films reported in literature [15], see Fig. 1b) and the transition width slightly increased. Both these effects are consistent with the fact that t approaches the coherence length of the material [15].

To perform EDL gating measurements, we covered the active channel and the gate counterelectrode placed on its side (made of a thin Au flake: see inset to Fig. 1a) with the liquid precursor of the cross-linked polymer electrolyte system (PES), which was later UV-cured.

To determine the surface electron density Δn_{2D} induced at the surface by a gate voltage V_G , we used the well-established electrochemical technique called Double-Step Chronocoulometry (DSCC) [14]. We applied a given V_G at room temperature (above the glass transition of the PES, which occurs below 230 K) as a step perturbation, and then removed it. As explained in Refs. [16], an analysis of the gate current (as a function of time) allowed us to separate the contribution to the current due to diffusion of electroreactants from that due to the EDL build-up; from the latter, we can determine the charge stored in the EDL and thus Δn_{2D} . A typical Δn_{2D} vs. V_G curve is shown in the inset to Fig.1b.

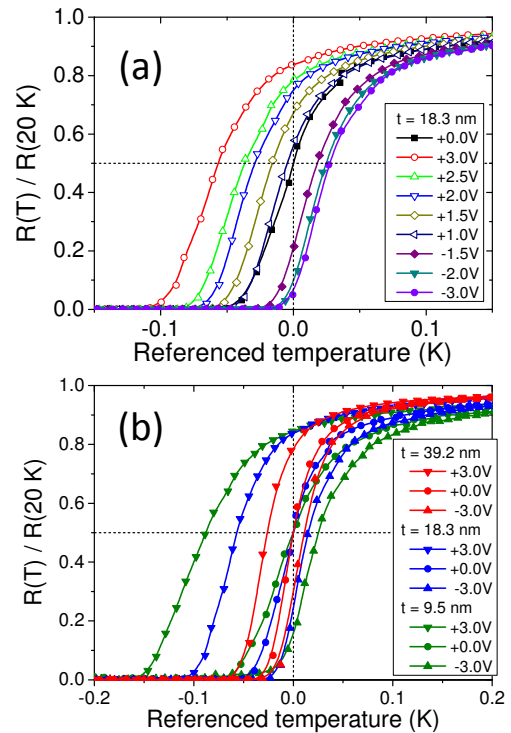


FIG. 2: (a) Normalized resistance $R(T)/R(20K)$ of the active channel of a 18.3 nm thick device, as a function of referenced temperature T^* , i.e. $T^* = [T^a - T_c^{ref}]_{V_G} - [T_c^a - T_c^{ref}]_0$, at different gate voltages in the range $[-3 V, +3 V]$. (b) Effect of a gate voltage $V_G = \pm 3V$ on the $R(T)/R(20K)$ vs. T^* curve for three values of thickness: 39.2 nm, 18.3 nm and 9.5 nm.

To measure the effect of a given V_G on the transition temperature, we applied V_G at room temperature and kept it constant while cooling the device down to 2.7 K in a pulse-tube cryocooler. Then, the voltage drops across the active and the reference channel, V_{active} and V_{ref} (see inset to Fig.1a) were measured simultaneously during the very slow, quasistatic heating up to room temperature in the presence of a source-drain dc current of a few μA .

The double-channel measurement allowed us to eliminate the possible small differences in critical temperature measured in different thermal cycles. By comparing the $R_{\square}(T)$ curve of the active channel with that of the reference channel measured at the same time, we were able to detect shifts in T_c due to gating as small as a few mK. For instance, the T_c shift due to a +3V gate voltage was evaluated as $\Delta T_c(3V) = [T_c^{active} - T_c^{ref}]_{V_G=3V} - [T_c^{active} - T_c^{ref}]_{V_G=0V}$.

Fig.2a shows, as an example, the effect of a gate voltage ranging between +3 V and -3 V in steps of 500 mV on the superconducting transition of the 18.3 nm thick film. The horizontal scale is the temperature normalized to the midpoint of the transition in the reference channel, i.e. $[T_c^{active} - T_c^{ref}]_{V_G} - [T_c^{active} - T_c^{ref}]_0$. As for all thicknesses, the gate voltage reproducibly produces a *rigid shift* of the superconducting transition to a lower

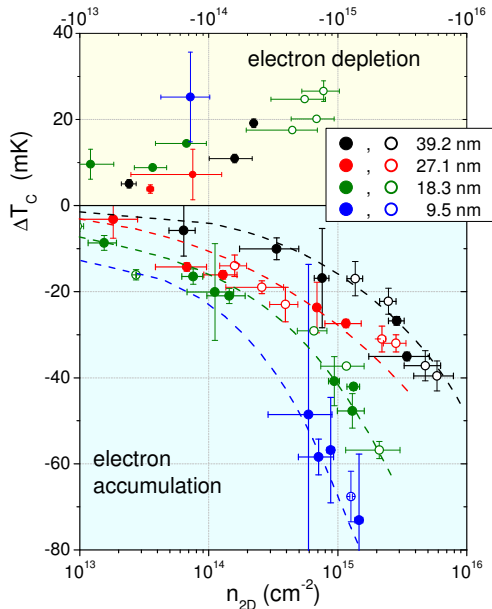


FIG. 3: T_c shift, ΔT_c , as a function of the induced surface electron density n_{2D} , for all the film thicknesses. Dashed lines are only guides to the eye.

(higher) temperature for positive (negative) V_G , respectively; the amplitude of the shift is clearly correlated with the induced charge density.

Figure 2b shows that the amplitude of the T_c shift produced by a given gate voltage (here +3.0 V and -3.0 V, corresponding to $\Delta n_{2D} = 2 \times 10^{15} \text{ cm}^{-2}$ and $-2 \times 10^{14} \text{ cm}^{-2}$, respectively) is greatly enhanced when the thickness t of the film is reduced. This fact (together with the detection of *negative* shifts of T_c for positive V_G) proves that the superconducting properties of the *whole* bulk are affected by the surface charge induction. The values of ΔT_c as a function of Δn_{2D} for the different thicknesses are summarized in Fig. 3c.

Interestingly, the transition width depends on the film thickness but *not* on the gate voltage, indicating that the charge induction does not create a T_c gradient in the depth of the film. The question then is how the electric field can homogeneously perturb the superconducting properties in the whole thickness even in the presence of a strong electronic screening.

In general, describing the electrostatic screening in a superconductor is a complicated task in which various aspects (including the degree of localization of the pairs) should play a role. But in the proximity of T_c the screening is dominated by unpaired electrons since the superfluid density is small. A two-fluid model in which the screening of Cooper pairs is calculated within the theory by Ovchinnikov [?] gives that, 100 mK below T_c (more than any shift we measured) the effective screening length is still 1.05 times the screening length of NbN in the normal state, i.e. about 0.5 Å.

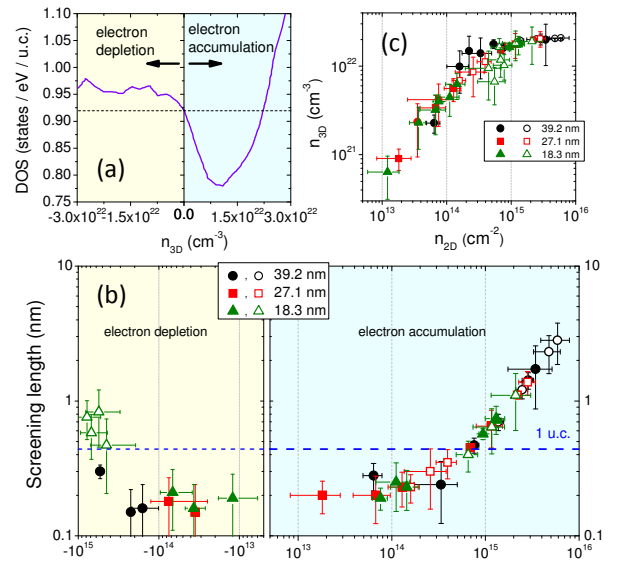


FIG. 4: (a) Density of states (DOS) of NbN as a function of the volume density of induced electrons Δn_{3D} (i.e. $\Delta n_{3D} = 0$ corresponds to native NbN, without gating). (b) Thickness of the perturbed surface layer d_s (that can be roughly assumed to be the screening length ξ_s) vs. Δn_{2D} for both electron accumulation and depletion. The horizontal dashed line indicates the size of one unit cell of NbN. (c) Absolute value of the volume density of induced electrons (in the surface layer) Δn_{3D} as a function of Δn_{2D} .

The most likely mechanism able to turn the perturbation of the carrier density in a thin surface layer into a homogeneous perturbation of the bulk superconducting properties is the proximity effect at a normal metal/superconductor interface— i.e. the induction of a superconducting order parameter in the normal bank (close to the interface) accompanied by its suppression in the superconducting one. For instance, in the case of electron accumulation, the surface layer has a T_c^s lower than the underlying bulk (T_c^b) and thus behaves as a thin normal slab between T_c^b and T_c^s .

Since NbN is well described by the BCS theory in the strong coupling regime, we can use the strong-coupling theory for proximity effect [13]. At low temperature, the coherence length of NbN is $\xi(0) \approx 4.5 \text{ nm}$, but close to the transition (let's say, for $(T_c^b - T) < 100 \text{ mK}$) $\xi(T) = \xi(0)/[1 - (T/T_c)^4] \geq 50 \text{ nm}$, so that the thickness of both the surface layer and of the underlying bulk are smaller than ξ . In these conditions, the model gives for the compound slab [13]:

$$\ln(T_{c,comp}) = \frac{\langle \lambda \ln(\Theta) \rangle}{\langle \lambda \rangle} - \frac{1}{\lambda^*} - \ln 1.45 \quad (1)$$

where Θ is a characteristic temperature, while

$$\lambda^* = \frac{[\langle \lambda \rangle - \mu^*]}{[1 + \langle \lambda \rangle]}, \quad (2)$$

$$\langle \lambda \rangle = \frac{\lambda_s N_s d_s + \lambda_b N_b d_b}{N_s d_s + N_b d_b} = \beta_s \lambda_s + \beta_b \lambda_b \quad (3)$$

$$\langle \lambda \ln \Theta \rangle = \beta_s \lambda_s \ln \Theta_s + \beta_b \lambda_b \ln \Theta_b. \quad (4)$$

Here, the subscripts s and b refer to surface and bulk, N_i is the density of states at the Fermi level and d_i the thickness of each layer, such that $d_s + d_b = t$. In a bulk superconductor eq. 1 reduces to a slightly simplified version of the McMillan equation $T_c = (\Theta/1.45) \exp(-1/\lambda^*)$. We assume that both Θ and the Coulomb pseudopotential μ^* are unaffected by the applied electric field and can thus be obtained from literature [INSERT REF]. As for the electron-phonon coupling strength λ_s , the simplest perturbation due to the induced charge density is $\lambda_s = \lambda_b \cdot N_s/N_b$, λ_b and N_b being calculated from the unperturbed T_c through the McMillan equation, and via density functional theory (DFT), respectively. The only remaining unknown quantity is the surface DOS at the Fermi level N_s . In general, the shift of the Fermi level is determined by the volume density of induced carriers Δn_{3D} , while DSCC is able to measure the surface charge density $\Delta n_{2D} = \int_0^t \Delta n_{3D}(z) dz$. An ansatz about how the volume charge density distributes across the thickness is thus required to determine N_s .

Since within the model in [13] the two layers of the compound slab are homogeneous, we choose a step profile for $\Delta n_{3D}(z)$, i.e. we assume the induced charge to be uniformly distributed in a thickness d_s , which is an adjustable parameter of the model. Clearly, d_s is connected to the screening length ξ_s even though it refers to a simplified step-like z -profile distribution of volume charges. For any given value of Δn_{2D} , the choice of d_s determines Δn_{3D} and consequently: i) the shift of the Fermi level at the surface; ii) the perturbed DOS at the surface, N_s ; iii) the electron-phonon coupling strength λ_s ; iv) the value of T_c^s , and finally the critical temperature of the compound slab $T_{c,comp}$ which has to agree with the experimental T_c .

The values of d_s (that we can take as the effective electrostatic screening length, EESL) that allow fitting the experimental T_c shifts, determined through an iterative procedure, are plotted as a function of Δn_{2D} in Fig. 4b. Symbols of different shape refer to different film thicknesses t [17]. It becomes immediately clear that the EESL does not depend on t , which is quite reasonable, but must vary with Δn_{2D} . Let us focus on the the electron accumulation side, where the trend is clearer. In the low-carrier density region, d_s roughly agrees with the Thomas-Fermi screening model if the density of quasiparticles present at $T \simeq T_c$ is used; but already at $7 \times 10^{14} \text{ cm}^{-2}$ it becomes as large as one unit cell (4.4 Å). Without this increase in d_s , the volume charge density Δn_{3D} would become so large that the Fermi level would be shifted well beyond the local minimum in the DOS (see Fig. 4a), resulting in an *increase* in the DOS N_s and thus in a *positive* ΔT_c , which is not the experimental result. For larger values of Δn_{2D} , d_s further expands, finally reaching 4-5 unit cells. For $\Delta n_{2D} > 5 \times 10^{14} \text{ cm}^{-2}$ the dependence of d_s on Δn_{2D} is remarkably linear. Note

that the increase in d_s is not fast enough to keep the volume density of induced electrons Δn_{3D} constant; indeed, this quantity increases as well, as shown in Figure 4c, and tends to saturate around $2 \times 10^{22} \text{ cm}^{-3}$.

These results indicate that the volume density of induced charges cannot exceed $2 \times 10^{22} \text{ cm}^{-3}$, and that the thickness of the surface layer departs from a Thomas-Fermi value (see fig. 4b) when Δn_{3D} approaches this limit (see fig.4a) as if the surface layer of thickness $\approx \lambda_{TF}$ was unable to accommodate all the induced charges. To look for an explanation of this effect, one certainly has to abandon the Thomas-Fermi approximation. In particular, for high densities of induced charge, the surface potential $\Phi(z=0)$ does no longer fulfill the condition $|e\Phi(z=0)| \ll E_F$ (i.e. it becomes as big as 300 meV for $V_G = 3 \text{ V}$) and the DOS cannot be considered constant when the Fermi level is shifted. The exact solution of the screening problem [?] qualitatively accounts for the observed increase in the EESL. In particular, the profile of $\Phi(z)$ in the metal (and thus of Δn_{3D}) is no longer a simple exponential (for instance, if $N(E)$ is a linearly decreasing function of E around E_F , $\Phi(z)$ is expressed by hyperbolic functions) and the spatial extension of the layer of charge induction is larger than in a Thomas-Fermi model. However, a quantitative disagreement persists. There is clearly a missing ingredient able to explain the limit in the volume density of charges, which is by far smaller than that due to Pauli's exclusion principle (controllare).

In summary, we have experimentally proven that a *surface* charge induction by electrochemical gating can give rise to modifications of the *bulk* superconducting properties (and not only of the surface ones). This is true, surprisingly, in conventional BCS-like superconductors with a large electronic screening, and can be explained in terms of proximity effect between the surface layer and the underlying part of the sample. We have also unveiled an increase in the effective electronic screening length, that departs from the Thomas-Fermi value and increases, suggesting the existence of an upper limit for the volume charge density.

These findings severely impact the study of the effects of EDL gating on high carrier density systems in general, and metallic superconductors in particular. On the one hand, they show the potential for EDL gating to affect the properties of a material well beyond the electric field screening length, allowing for the control of order parameters also in bulk-like systems. On the other hand, they pose strong limits on the investigation of pure surface-limited modulations in these systems, as ultrathin films of few unit cells at most will be required to completely avoid the influence of proximity effects in the experiments.

* Electronic address: renato.gonnelli@polito.it

- [1] S. Jo, D. Costanzo, H. Berger, and A.F. Morpurgo, *Nano Lett.* **15** 1197 (2015)
- [2] K. Ueno et al., *Nature Materials* **7**, 855 (2008)
- [3] J.T. Ye, Y.J. Zhang, R. Akashi, M. S. Bahrany, R. Arita and Y. Iwasa, *Science* **338**, 1193 (2012).
- [4] J. T. Ye, S. Inoue, K. Kobayashi, Y. Kasahara, H. T. Yuan, H. Shimotani and Y. Iwasa, *Nature Materials* **9**, 125 (2010)
- [5] K. Ueno, S. Nakamura, H. Shimotani, H. T. Yuan, N. Kimura, T. Nojima, H. Aoki, Y. Iwasa and M. Kawasaki, *Nature Nanotechnology* **6**, 408 (2011).
- [6] D. Daghero, F. Paolucci, A. Sola, M. Tortello, G. A. Ummarino, M. Agosto, R. S. Gonnelli, Jijeesh R. Nair, and C. Gerbaldi, *Phys Rev. Lett.* **108**, 066807 (2012)
- [7] H. Nakayama, J. Ye, T. Ohtani, Y. Fujikawa, K. Ando, Y. Iwasa, E. Saitoh, *Appl. Phys. Expr.* **5**, 023002 (2012)
- [8] M. Tortello, A. Sola, Kanudha Sharda, F. Paolucci, J.R. Nair, C. Gerbaldi, D. Daghero, R.S. Gonnelli, *Appl. Surf. Sci.* **269**, 17 22 (2013)
- [9] R.E. Glover and M. D. Sherrill, *Phys. Rev. Lett.* **5**, 248 (1960)
- [10] H. L. Stadler, *Phys. Rev. Lett.* **14**, 979 (1965)
- [11] J. Choi, R. Pradheesh, H. Kim, H. Im, Y. Chong, and D.-H. Chae, *Appl. Phys. Lett.* **105**, 012601 (2014)
- [12] A. Nigro et al., *Phys. Rev. B* **37**, 3970 (1998)
- [13] W. Silvert, *Phys. Rev. B* **12**, 4870 (1975)
- [14] G. Inzelt, in *Electroanalytical Methods. Guide to Experiments and Applications 2nd edn.* (ed Scholz, F.), Ch. II.4 Chronocoulometry, 147-158 (Springer-Verlag, 2010)
- [15] Z. Wang, A. Kawakami, Y. Uzawa, and B. Komiyama, *J. Appl. Phys.* **79**, 7838 (1996)
- [16] E. Piatti, A. Sola, D. Daghero, G. A. Ummarino, F. Laviano, J. R. Nair, C. Gerbaldi, R. Cristiano, A. Casaburi, and R. S. Gonnelli, *J. Supercond. Nov. Magn.* **29**, 587591 (2016)
- [17] We excluded from our analysis the data for $t = 9.5$ nm as we deem the measured T_c shift not to be reliable enough due to the strong hysteresis of the field effect (see Supplementary Material for details).